

Fermionic Vacuum Energy from a Nielsen-Olesen Vortex

M. BORDAG*

and

I. Drozdov†

University of Leipzig, Institute for Theoretical Physics
Augustusplatz 10/11, 04109 Leipzig, Germany

October 18, 2018

Abstract

We calculate the vacuum energy of a spinor field in the background of a Nielsen-Olesen vortex. We use the method of representing the vacuum energy in terms of the Jost function on the imaginary momentum axis. Renormalization is carried out using the heat kernel expansion and zeta functional regularization. With this method well convergent sums and integrals emerge which allow for an efficient numerical calculation of the vacuum energy in the given case where the background is not known analytically but only numerically. The vacuum energy is calculated for several choices of the parameters and it turns out to give small corrections to the classical energy.

1 Introduction

Quantum corrections to classical background configurations are a topic of continuing interest. At present it is stimulated by the observation made in lattice calculations that the field configurations responsible for confinement are dominated by monopole or string like configurations. Another motivation comes from the stability analysis of Z-strings with respect to fermionic fluctuations.

During the last years quantum corrections to string like configurations have been investigated quite actively. In [1] for the background of a finite radius magnetic flux tube in QED the vacuum energy of a spinor was calculated. There

*e-mail: Michael.Bordag@itp.uni-leipzig.de

†e-mail: Igor.Drozdov@itp.uni-leipzig.de

the method of representing the vacuum energy in terms of the Jost function of the related scattering problem taken on the imaginary momentum axis was applied. This method has been developed earlier in [2] for spherically symmetric scalar background fields. The specific example considered in [1] was a homogeneous magnetic field inside the flux tube. This investigation was extended to more complicated profiles of the magnetic field inside the flux tube in [3, 4]. In [5] a magnetic background was considered which depends only on one spatial coordinate. In addition, this dependence is of a form that the corresponding wave equation has an explicit solution so that the vacuum energy could be calculated quite easily. A more general approach to fermionic vacuum energy was taken in [6] where general bounds on the fermionic determinant were obtained. Another approach was taken in [7] where several profiles of the magnetic background were considered and compared with the derivative expansion. In [8] the limit of a strong magnetic field was investigated in more detail.

There is still an interest in backgrounds of infinitely thin strings which constitute a singular background. Typical for these configurations is the need to apply the method of self adjoint extensions. The object to consider in such examples is the vacuum energy density per unit volume rather than the 'global' vacuum energy which is for a string the density per unit length. For recent investigations see, for example, [9] and [10]. The problem with infinitely thin strings is that their classical energy is infinite. Also, there are additional counter terms. In the language of heat kernel expansion there are additional contributions to the heat kernel coefficients, for instance coefficients with half integer number, which reside on the surface where the singularity is located. Another related example was considered in [3] where the background is a finite radius flux tube with the magnetic field concentrated on the surface of the string. The advantage of singular (and non smooth like in [1]) backgrounds can be seen in the usually quite explicit formulas for the quantum fluctuations. So in [9, 10, 3] only Bessel functions appear and in [1, 4] hyper geometric functions in addition.

In general, physical background configurations should have a finite energy, hence strings should have a non zero radius. A typical example is the Nielsen-Olesen string [11]. But here, not only the vacuum fluctuations have to be calculated numerically, but even the background itself. The problem appears to have a calculational scheme which does not need explicit formulas and which allows for efficient numerical evaluation. There the main problem comes from the ultraviolet divergencies. In analytical terms it is well known how to handle them. First one has to introduce some intermediate regularization. After that one has to subtract the counter terms and finally to remove the regularization resulting now in a finite result. However, consider the last step in zeta functional regularization. Here one has to perform an analytical continuation. Or let us consider some cut-off regularization, where one has to remove the contributions proportional to non negative powers of the cut-off parameter. In principle such a procedure can be done numerically (there are some examples) but this is quite complicated and

ineffective. It is better to transform the expression for the vacuum energy in a way that the final removal of the regularization can be performed analytically so that only well convergent sums and integrals remain. Such a method had been developed in [12, 2] and in [1, 13] applied to strings of finite radius. The method is based on a representation of the regularized vacuum energy in terms of the Jost function of the related scattering problem taken on the imaginary momentum axis. Another method, using phase shifts and momenta on the real axis was used in [14] (see also [15] and references therein), mainly for spherically symmetric backgrounds. Also, using phase shifts, the case of a color magnetic vortex was considered in [16]. In a similar way in [17] the vacuum energy for an electroweak string had been considered, where, however, a step profile was taken in the final stage.

A completely different method is worth to be mentioned. In [18, 19] world line methods were applied to the calculation of vacuum energy which have the advantage not to rely on separation of variables and therefore to be applicable for much more general background configurations.

In the present paper we calculate the vacuum energy of a fermion in the background of a Nielsen-Olesen string. We use the method of representing the regularized vacuum energy in terms of the Jost function on the imaginary momentum axis which was developed in [2]. For the Nielsen-Olesen vortex the background potential is given only as a numerical solution of the corresponding equations of motion. We use zeta functional regularization and determine the counter terms from standard heat kernel expansion. The renormalized vacuum energy is divided into two parts, the 'finite' and the asymptotic ones, by subtraction and addition of some first terms of the uniform asymptotic expansion of the Jost function which is obtained using the Lipmann-Schwinger equation. In the asymptotic part the analytic continuation in the regularization parameter is performed analytically and well convergent double integrals remain. The 'finite' part is represented as a well convergent sum and integral involving the Jost function which is calculated from the numerical solutions of the corresponding wave equation. Using these tools, the dependence on the parameters of the considered model is investigated numerically.

The paper is organized as follows. In the next section the basic notations for the considered model are introduced, the renormalization is discussed and the basic formulas for the representation of the vacuum energy are given. In the third section the asymptotic part of the Jost function is derived and the asymptotic part of the vacuum energy as well. In the fourth section the 'finite' part of the vacuum energy is derived and the convergence properties are discussed. Sect. 5 contains the numerical part of the work and Sect. 6 the conclusions.

We use units where $\hbar = c = 1$.

2 Basic notations

The Abelian Higgs model contains a $U(1)$ gauge field, $A_\mu(x)$, and a complex scalar field, $\Phi(x)$. The action is

$$S = \int d^4x \left(-\frac{1}{4}F_{\mu\nu}^2 + |D_\mu\Phi|^2 - \lambda \left(|\Phi|^2 - \frac{\eta^2}{2} \right)^2 \right), \quad (1)$$

where $D_\mu = \partial_\mu - iqA_\mu$ is the covariant derivative and $F_{\mu\nu} = \partial_\mu A_\nu - \partial_\nu A_\mu$ is the field strength, for more details see [20]. The vacuum configuration is given by $A_\mu = 0$, $\Phi = \eta e^{ic}/\sqrt{2}$ where c is some constant and η is the Higgs condensate. This configuration has zero energy. A configuration with finite non zero energy must be at spatial infinity in the vacuum manifold. Hence asymptotically the gauge potential must be a pure gauge and the scalar field must tend to a constant times an angular dependent phase. A configuration of such type is the Nielsen-Olesen string [11]. In cylindrical coordinates $(x, y, z) \rightarrow (r, \varphi, z)$ one makes the ansatz

$$\Phi = \frac{\eta}{\sqrt{2}}f(r)e^{in\varphi}, \quad qA_\varphi = nv(r), \quad (2)$$

where A_φ is the angular component of the vector potential. The profile functions satisfy the boundary conditions

$$f(0) = v(0) = 0, \quad f(r) \rightarrow 1, v(r) \rightarrow 1 \text{ as } r \rightarrow \infty. \quad (3)$$

Here n is the winding number and gives at once the magnetic flux in the string. In the following we consider $n = 1$ only. The equations of motion imply

$$\begin{aligned} f''(r) + \frac{1}{r}f'(r) - \frac{1}{r^2}(1 - v(r))^2 f(r) + \lambda\eta^2(1 - f(r)^2) f(r) &= 0, \\ v''(r) - \frac{1}{r}v'(r) + q^2\eta^2 f(r)^2(1 - v(r)) &= 0. \end{aligned} \quad (4)$$

After a rescaling, $r = \rho/(q\eta)$, these equations depend in fact only on the combination $\beta = 2\lambda/q^2$, which is at once the squared ratio of the Higgs and vector masses. For $\beta = 1$ the system exhibits an additional symmetry and can be reduced to two first order equations (Bogomolny equations). For $\beta < 1$ the system is stable for all values of the flux $n = 1, 2, \dots$, for $\beta > 1$ only $n = 1$ is stable (a vortex with $n > 1$ decays into n vortexes with $n = 1$).

The system of equations (4) together with the boundary conditions (3) does not have an analytical solution and one is left with numerical methods. The simplest way is to set the derivatives in zero, i.e. the constants a and b the expansion for small r , $f(r) = ar + \dots$ and $v(r) = br^2 + \dots$, and to numerically integrate the equations from $r = 0$ to larger values of r . One has to adjust these constants in a way that for large r the asymptotic values $f = 1$ and $v = 1$ are approached. Examples are shown in Fig. 1 for two values of β with $q\eta = 1$. The

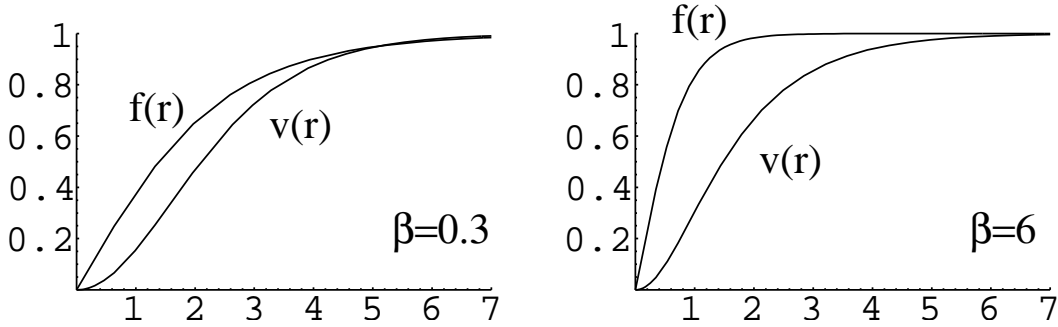


Figure 1: The profile functions of the Nielsen-Olesen vortex as functions of the radius r for $q\eta = 1$.

corresponding values of the derivatives are $(a, b) = (0.26817, 0.17481)$ for $\beta = 0.3$ and $(a, b) = (0.79958, 0.42848)$ for $\beta = 6$. As the asymptotic values for $r \rightarrow \infty$ are reached with exponential speed it is in fact sufficient to consider r up to ≈ 15 .

The classical energy (more exactly, the energy density per unit length) of these configurations is given by

$$E_{\text{class}} = \pi \int_0^\infty dr r \left(\frac{1}{q^2 r^2} v'(\rho)^2 + \eta^2 \left(f'(\rho)^2 + \frac{1}{r^2} (1 - v(\rho))^2 f(\rho)^2 \right) + \frac{\lambda}{2} \eta^4 (1 - f(\rho)^2)^2 \right). \quad (5)$$

We calculate the background for $q\eta = 1$ and restore later the general setting by inserting $\rho = q\eta r$ in (5).

The spinor is taken as a four component Dirac spinor with a coupling to the background given by the Lagrange density

$$L = -i\bar{\Psi} (i\gamma^\mu D_\mu - f_e |\Phi|) \Psi. \quad (6)$$

This model is chosen for the reason of simplicity. It provides a coupling of the spinor not only to the vector but also to the scalar background and it is motivated by the Yukawa coupling in the fermionic sector of the standard model. We note that the interaction in (6) is gauge invariant and that the coupling constant f_e is dimensionless. However, this model has a drawback. Since there is only one spinor we are forced to take the absolute value, $|\Phi| = \sqrt{(\Re\Phi)^2 + (\Im\Phi)^2}$, of the complex scalar field (in the standard model there we don't need to do so). As a consequence, the interaction is non polynomial. This is a complication, for example if considering the vacuum energy together with the dynamics of the background. Also, there is a need for an additional counter term (see below). However, because we are not going to consider the dynamics of the background, this complication does not affect the calculation of the vacuum energy if we let

enter the additional counter terms into the classical energy with a coefficient which is put equal to zero after the renormalization is carried out. In addition, if we consider the same problem of calculating the vacuum energy in the standard model then there is no such complication due to its renormalizability.

The background is static and due to the translational invariance in direction along the z -axis and the rotational invariance around the z -axis ($m = 0, \pm 1, \dots$ is the orbital angular momentum), the corresponding momenta can be separated, $\Psi \rightarrow e^{-ip_0x^0 + ip_3x^3} \begin{pmatrix} \Psi_1 e^{-(m+1)\varphi} \\ \Psi_2 e^{-m\varphi} \end{pmatrix}$. After that the Dirac equation decouples and one of the resulting pair of two component equations may be represented as

$$\begin{pmatrix} p_0 - \mu(r) & , & \frac{\partial}{\partial r} - \frac{m-v(r)}{r} \\ -\frac{\partial}{\partial r} - \frac{m+1-v(r)}{r} & , & p_0 + \mu(r) \end{pmatrix} \begin{pmatrix} \Psi_1 \\ \Psi_2 \end{pmatrix} = 0. \quad (7)$$

The other pair is obtained by changing the sign of μ . Here the notation $\mu(r) = f_e \frac{\eta}{\sqrt{2}} f(r)$ has been introduced. With respect to the spinor this is a radius dependent mass density. From its value at infinity we define the spinor mass, $m_e = f_e \frac{\eta}{\sqrt{2}}$. For a constant mass density the problem is the same as for a pure magnetic flux tube which appears as a special case in this way.

The vacuum energy of the spinor is given by the general formula

$$\mathcal{E}_{\text{quant}} = -\frac{1}{2} \sum_{(n)} e_{(n)}^{1-2s}. \quad (8)$$

Here s is the zeta functional regularization parameter and $e_{(n)}$ are the one particle energies. For simplicity we dropped the arbitrary constant μ which is usually introduced to adjust the dimension in zeta functional regularization. The quantum numbers (n) include the sign of the one particle energies (all enter with positive sign), the spin s_z (two projections which we can account for by summing over the sign of $\mu(r)$), the orbital angular quantum number m and the radial quantum number n_r (assuming for a moment the system being inserted into a large cylinder). In addition there is the momentum p_3 which can be integrated according to

$$\int_{-\infty}^{\infty} \frac{dp_3}{2\pi} (p_3^2 + x^2)^{\frac{1}{2}-s} = x^{2(1-s)} \frac{\Gamma(s-1)}{2\sqrt{\pi}\Gamma(s-\frac{1}{2})} = x^{2(1-s)} \frac{C_s}{4\pi s}$$

with $C_s = 1 + s(2 \ln 2 - 1) + \dots$ and we arrive at

$$\mathcal{E}_{\text{quant}} = -\frac{C_s}{4\pi s} \sum_{s_z, m, n_r} (e_{s_z, m, n_r})^{2(1-s)}. \quad (9)$$

In order to get rid of the large cylinder we proceed as in [1]. We consider the cylindrical scattering problem associated with Eq. (7) and define the Jost functions, $f_m(k)$, with $p_0 = \sqrt{m_e^2 + k^2}$. We rewrite the sum over n_r by an integral, then the

large cylinder to infinity and after dropping the Minkowski space contribution we end up with

$$\mathcal{E}_{\text{quant}} = \frac{C_s}{4\pi} \sum_{\text{sgn}\mu} \sum_{m=-\infty}^{\infty} \int_{m_e}^{\infty} dk \left(k^2 - m_e^2\right)^{1-s} \frac{\partial}{\partial k} \ln f_m(ik) \quad (10)$$

which is our expression for the regularized ground state energy. Here the integration is turned to the imaginary axis, more specifically, it goes along the cut resulting from $(k^2 - m_e^2)^{1-s}$. In order to fully exploit the symmetry we renumber the orbital momenta by ν according to

$$m = \begin{cases} \nu - \frac{1}{2} & (m \geq 0) \\ -\nu - \frac{1}{2} & (m < 0) \end{cases} \quad (11)$$

with $\nu = \frac{1}{2}, \frac{3}{2}, \dots$ and two signs of the orbital momentum are to be taken into account. After rotation $k \rightarrow ik$ we define $p = \sqrt{k^2 - m_e^2}$ and for positive orbital momentum Eq. (7) can be rewritten in the form

$$\begin{pmatrix} ip - \mu(r) & , & \frac{\partial}{\partial r} - \frac{\nu-1/2-v(r)}{r} \\ -\frac{\partial}{\partial r} - \frac{\nu+1/2-v(r)}{r} & , & ip + \mu(r) \end{pmatrix} \begin{pmatrix} \Psi_1 \\ \Psi_2 \end{pmatrix} = 0. \quad (12)$$

It can be seen (see below, Eqs. (44) and (45)) that for the Jost function a change in the sign of μ corresponds to complex conjugation and a change in the sign of the magnetic background, $v(r) \rightarrow -v(r)$, corresponds to an exchange of positive and negative orbital momenta. As a consequence, in Eq. (10) we have a factor of 4 and we take the real part of the half sum of positive and negative orbital momenta.

The next step is the renormalization. We use the standard heat kernel expansion according to which the divergent part of the ground state energy is given by (see, e.g., [1] and we drop a_0)

$$E^{\text{div}} = \frac{m_e^2}{32\pi^2} \left(\frac{1}{s} + \ln \frac{4}{m_e^2} - 1 \right) a_1 - \frac{1}{32\pi^2} \left(\frac{1}{s} + \ln \frac{4}{m_e^2} - 2 \right) a_2, \quad (13)$$

where a_i are the standard heat kernel coefficients. We define the renormalized ground state energy by $s \rightarrow 0$

$$E_{\text{ren}} = \mathcal{E}_{\text{quant}} - E^{\text{div}} \quad (14)$$

in the limit $s \rightarrow 0$. The definition (14) of the renormalized ground state energy is chosen in a way that E_{ren} vanishes if the spinor mass m_e taken as a parameter independent from the background becomes large. This is the so called 'large mass' normalization condition. It has been discussed in detail in [22, 23] and in [24] it was shown to be equivalent to the known 'no tadpole' condition.

The heat kernel coefficients can be calculated using known methods from the squared Dirac operator,

$$\begin{aligned} (i\mathcal{D} + \mu(r))(i\mathcal{D} - \mu(r)) &= -D^2 + \frac{q}{2}F_{\mu\nu}\sigma^{\mu\nu} - if_e\gamma^\mu \frac{\partial}{\partial x^\mu} |\Phi| - f_e^2 |\Phi|^2 \\ &\equiv -D^2 + V \end{aligned} \quad (15)$$

with $\sigma^{\mu\nu} = \frac{i}{2}[\gamma^\mu, \gamma^\nu]$. The general expressions for the relevant heat kernel coefficients are

$$\begin{aligned} a_1 &= \text{Tr} \int d^2x (-V), \\ a_2 &= \text{Tr} \int d^2x \left(-\frac{1}{12}F_{\mu\nu}^2 + \frac{1}{2}V^2 - \frac{1}{6}\Delta V \right), \end{aligned} \quad (16)$$

where the trace is over the gamma matrices. Inserting for V the result is

$$\begin{aligned} a_1 &= -8\pi \int_0^\infty dr r (\mu(r)^2 - m_e^2), \\ a_2 &= 8\pi \int_0^\infty dr r \left(\frac{1}{3} \frac{v'(r)^2}{r^2} + \frac{1}{2} (\mu'(r)^2 + (\mu(r)^2 - m_e^2)^2) \right) \end{aligned} \quad (17)$$

(note that we consider densities per unit length of the string). From Eq. (13) we obtain the divergent part of the vacuum energy in the form

$$\begin{aligned} \mathcal{E}^{\text{div}} &= -\frac{1 - 2s(\ln(m_e/2) + 1)}{4\pi s} \int_0^\infty dr r \left(\frac{1}{3} \frac{v'(r)^2}{r^2} + \frac{f_e^2 \eta^2}{4} f'(r)^2 \right. \\ &\quad \left. + \frac{f_e^4 \eta^4}{8} (f(r)^4 - 1) \right) - \frac{1}{4\pi} \int_0^\infty dr r \frac{f_e^4 \eta^4}{4} (f(r)^2 - 1) + O(s). \end{aligned} \quad (18)$$

The interpretation is as follows. From the $v'(r)^2$ -term we have the standard renormalization of the electric charge q in the classical action (5). A renormalization of the scalar coupling λ absorbs the divergence proportional to $f(r)^4$. After that the remaining freedom is in a change of the condensate η . However, this is obviously insufficient to absorb the remaining parts of \mathcal{E}^{div} . In this way, in the classical energy an additional structure must be present. As suggested from Eq. (15), it is necessary to introduce at last a term proportional to $\left(\frac{\partial}{\partial x^\mu} |\Phi|\right)^2$ into the action (1) and into the classical energy (5) as well. It should be noted that such a term is gauge invariant and that it has the correct dimension. However, it represents another non polynomial interaction. This is not surprising as the model given by Eq. (6) itself contains a non polynomial interaction. Accepting this we can finish the renormalization if we put the coefficient in front of this term equal to zero after performing the renormalization.

In order to perform the limit $s \rightarrow 0$ in Eq. (14) we need to rewrite the regularized ground state energy. For this we define the asymptotic Jost function as the part of its uniform asymptotic expansion for $\nu \rightarrow \infty$, $z \equiv \frac{k}{\nu}$ fixed, which includes all powers up to ν^{-3} ,

$$\ln f_\nu(ik) = \ln f_\nu^{\text{as}} + O\left(\frac{1}{\nu^4}\right). \quad (19)$$

Using $\ln f_\nu^{\text{as}}$ we divide the energy into

$$E_{\text{ren}} = \mathcal{E}_f + E^{\text{as}} \quad (20)$$

with the 'finite' part,

$$\mathcal{E}^f = \frac{1}{\pi} \sum_{\nu=\frac{1}{2}, \frac{3}{2}, \dots} \int_{m_e}^{\infty} dk \left(k^2 - m_e^2\right) \frac{\partial}{\partial k} (\ln f_\nu(ik) - \ln f_\nu^{\text{as}}(ik)) \quad (21)$$

and the 'asymptotic' part,

$$E^{\text{as}} = \frac{1}{\pi} \sum_{\nu=\frac{1}{2}, \frac{3}{2}, \dots} \int_{m_e}^{\infty} dk \left(k^2 - m_e^2\right)^{2(1-s)} \frac{\partial}{\partial k} \ln f_\nu^{\text{as}}(ik) - E^{\text{div}}. \quad (22)$$

The sum and the integral in \mathcal{E}^f , Eq. (21), are finite by construction of the asymptotic Jost function. Therefore we could put $s = 0$ therein. In the asymptotic part, E^{as} , Eq. (22), the analytic continuation in s has to be still performed which will be done in the next section.

3 The asymptotic part of the vacuum energy

The asymptotic part of the Jost function can be derived from the Lipmann-Schwinger equation just generalizing the procedure developed in [1]. The operator $\Delta\mathcal{P}$ there in Eq. (28) reads now

$$\Delta\mathcal{P} = \begin{pmatrix} \mu(r) & , & -\frac{v(r)}{r} \\ -\frac{v(r)}{r} & , & -\mu(r) \end{pmatrix}. \quad (23)$$

Again, we have to perform iterations up to the fourth order in the operator $\Delta\mathcal{P}$. Using the formulas given in [1] one arrives at the representation

$$\ln f_\nu^{\text{as}}(ik) = \int_0^\infty \frac{dr}{r} \sum_{n=1}^3 \sum_{j=n}^{3n} X_{nj} \frac{t^j}{\nu^n} \quad (24)$$

with $t = \frac{1}{\sqrt{1+(\nu z)^2}}$. The coefficients are

$$\begin{aligned}
X_{11} &= \frac{1}{2}v(r)^2 + \frac{1}{2}r^2(\mu(r)^2 - m_e^2), \\
X_{13} &= -\frac{1}{2}v(r)^2, \\
X_{33} &= \frac{1}{4}v(r)^2 - \frac{1}{8}r^2v'(r)^2 - \frac{1}{8}v(r)^4 - \frac{1}{4}r^2v(r)^2(\mu^2 - m_e^2) \\
&\quad - \frac{1}{8}r^4(\mu'(r)^2 + (\mu^2 - m_e^2)^2), \\
X_{35} &= -\frac{39}{16}v(r)^2 + \frac{1}{8}r^2v'(r)^2 + \frac{3}{4}v(r)^4 + \frac{3}{4}r^2v(r)^2(\mu^2 - m_e^2) - \frac{3}{16}r^2(\mu^2 - m_e^2), \\
X_{37} &= \frac{35}{8}v(r)^2 - \frac{5}{8}v(r)^4 + \frac{5}{16}r^2(\mu^2 - m_e^2), \\
X_{39} &= -\frac{35}{16}v(r)^2. \tag{25}
\end{aligned}$$

The dependence on $v(r)$ is the same as in [1] (where it was denoted by $a(r)$), the dependence on $\mu(r)$ is new. In Eq. (24) it had been integrated by parts in order to get the shortest representation for the coefficients X_{nj} .

In \mathcal{E}^{as} , Eq. (22), the analytic continuation in s can be performed by rewriting the sum over the orbital momenta ν by integrals using the Abel-Plana formula in the form as given in the Appendix, Eq. (53). From the first part, i.e., from the direct integral over ν , we get a contribution which just cancels E^{div} in Eq. (22). So we are left with the contribution from the second part. Here we integrate over k using the simple formula (54) and obtain

$$\mathcal{E}^{\text{as}} = -\frac{C_s}{\pi} m_e^{2(1-s)} \int_0^\infty \frac{dr}{r} \sum_{n,j} X_{nj} \frac{\Gamma(2-s)\Gamma(s+\frac{j}{2}-1)}{\Gamma(j/2)} \Sigma_{nj}(rm_e) \tag{26}$$

with

$$\Sigma_{nj}(x) = \frac{1}{x^j} \int_0^\infty \frac{d\nu}{1+e^{2\pi\nu}} \frac{1}{i} \left(\frac{(i\nu)^{j-n}}{\left(1+\left(\frac{i\nu}{x}\right)^2\right)^{s+j/2-1}} - \frac{(-i\nu)^{j-n}}{\left(1+\left(\frac{-i\nu}{x}\right)^2\right)^{s+j/2-1}} \right). \tag{27}$$

The difference in the right hand side results from the deformation of the integration contour in the Abel-Plana formula which gets tight around the cut. Therefore the integration starts effectively from $\nu = x$. This formula provides the best representation to perform the analytic continuation in s . For $(n, j) = (1, 1)$ we simply note

$$\Sigma_{11}(x) = \frac{2}{x^2} \int_x^\infty d\nu \frac{1}{1+e^{2\pi\nu}} \sqrt{\nu^2 - x^2}. \tag{28}$$

Also for $(n, j) = (1, 3)$ we can put $s = 0$ immediately. However, we prefer to integrate by parts in order to get a representation which is in line with Eq. (28).

In a similar way, integrating by parts, we can proceed in all other contributions. So the final form is

$$\Sigma_{nj}(x) = \frac{2}{x^2} \int_x^\infty d\nu f_{nj}(\nu) \sqrt{\nu^2 - x^2} \quad (29)$$

with

$$\begin{aligned} f_{11}(\nu) &= \frac{1}{1+e^{2\pi\nu}}, & f_{13}(\nu) &= -\left(\frac{\nu}{1+e^{2\pi\nu}}\right)', \\ f_{33}(\nu) &= \left(\frac{1}{\nu(1+e^{2\pi\nu})}\right)', & f_{35}(\nu) &= \left(\frac{1}{\nu}\left(\frac{\nu}{1+e^{2\pi\nu}}\right)'\right)', \\ f_{37}(\nu) &= \frac{1}{3}\left(\frac{1}{\nu}\left(\frac{1}{\nu}\left(\frac{\nu^3}{1+e^{2\pi\nu}}\right)'\right)'\right)', & f_{39}(\nu) &= \frac{1}{15}\left(\frac{1}{\nu}\left(\frac{1}{\nu}\left(\frac{1}{\nu}\left(\frac{\nu^5}{1+e^{2\pi\nu}}\right)'\right)'\right)'\right)'. \end{aligned}$$

Using these formulas in Eq. (26) we can put $s = 0$ there and insert for the coefficients X_{nj} using Eqs.(25). After rearranging contributions we arrive at

$$\begin{aligned} \mathcal{E}^{\text{as}} &= \frac{-2}{\pi} \int_0^\infty \frac{dr}{r^3} \left(v(r)^2 h_1(rm_e) + r^2 v'(r)^2 h_2(rm_e) + v(r)^4 h_3(rm_e) \right. \\ &\quad \left. + r^2 v(r)^2 (\mu(r)^2 - m_e^2) h_4(rm_e) + r^2 (\mu(r)^2 - m_e^2) h_5(rm_e) \right. \\ &\quad \left. + r^4 (\mu'(r)^2 + (\mu(r)^2 - m_e^2)^2) h_6(rm_e) \right) \end{aligned} \quad (30)$$

with

$$h_j(x) = \int_x^\infty d\nu f_j(\nu) \sqrt{\nu^2 - x^2} \quad (31)$$

and

$$\begin{aligned} f_1(\nu) &= -f_{11}(\nu) - f_{13}(\nu) + \frac{1}{2}f_{33}(\nu) - \frac{13}{8}f_{35}(\nu) + \frac{7}{4}f_{37}(\nu) - \frac{5}{8}f_{39}(\nu), \\ f_2(\nu) &= -\frac{1}{4}f_{33}(\nu) + \frac{1}{12}f_{35}(\nu), \\ f_3(\nu) &= -\frac{1}{4}f_{33}(\nu) + \frac{1}{2}f_{35}(\nu) - \frac{1}{4}f_{37}(\nu), \\ f_4(\nu) &= -\frac{1}{2}f_{33}(\nu) + \frac{1}{2}f_{35}(\nu), \\ f_5(\nu) &= -f_{11}(\nu) - \frac{1}{8}f_{35}(\nu) + \frac{1}{8}f_{37}(\nu), \\ f_6(\nu) &= -\frac{1}{4}f_{33}(\nu). \end{aligned} \quad (32)$$

According to these functions we divide the asymptotic part of the ground state energy,

$$\mathcal{E}^{\text{as}} \equiv \sum_{j=1}^6 \mathcal{E}_j^{\text{as}}, \quad (33)$$

into parts which have the meaning, for instance, of the asymptotic part of the vacuum energy resulting from the magnetic background, $\mathcal{E}_1^{\text{as}}$, $\mathcal{E}_2^{\text{as}}$ and $\mathcal{E}_3^{\text{as}}$, or

from the mixed contribution, $\mathcal{E}_4^{\text{as}}$, etc. We finish this section with the remark, that the integrals in Eq. (30) are all finite for the considered background of a Nielsen-Olesen vortex due to corresponding properties of the functions $h_i(x)$, their behavior at $x \rightarrow 0$ for instance.

4 The 'finite' part of the vacuum energy and numerical results

In order to calculate the finite part of the vacuum energy defined by Eq. (21) we have, first of all, to set up a numerical scheme for the calculation of the Jost function. The Jost function is defined as the coefficients in the asymptotics for large radius in the so called regular solution of the wave equation (7),

$$\Psi^{(\pm)}(r) \sim \frac{1}{2} \left\{ f_\nu^{(\pm)}(k) \Psi_{H^{(2)}}^{(\pm)}(kr) + \bar{f}_\nu^{(\pm)}(k) \Psi_{H^{(1)}}^{(\pm)}(kr) \right\}, \quad (34)$$

where

$$\Psi_{H^{(1,2)}}^{(\pm)}(kr) = \begin{pmatrix} \sqrt{p_0 + m_e} H_{\nu \pm (\frac{1}{2} - \delta)}^{(1,2)}(kr) \\ \pm \sqrt{p_0 - m_e} H_{\nu \mp (\frac{1}{2} + \delta)}^{(1,2)}(kr) \end{pmatrix} \quad (35)$$

($p_0 = \sqrt{m_e^2 + k^2}$) are the two linear independent solutions at $r \rightarrow \infty$. The signs (\pm) correspond to the sign of the orbital momentum according to Eq. (11) and $H_\mu^{(1,2)}(z)$ are Hankel functions. In general, δ is the dimensionless value of the magnetic flux, i.e. it is $v(r \rightarrow \infty)$, which is equal to one in our case.

From Eq. (34), the Jost function can be expressed in terms of the solutions,

$$f_\nu^{(\pm)}(k) = \frac{\pi r}{2i} \left(\mp \sqrt{p_0 - m_e} \psi_1(r) H_{\nu \mp (\frac{1}{2} + \delta)}^{(1)}(kr) + \sqrt{p_0 + m_e} \psi_2(r) H_{\nu \pm (\frac{1}{2} - \delta)}^{(1)}(kr) \right), \quad (36)$$

where $\psi_{1,2}(kr)$ are the upper and lower components of $\Psi(r)$. Strictly speaking, as given by Eq. (36), the functions $f_\nu^{(\pm)}(k)$ depend on r and only for $r \rightarrow \infty$ they tend to the Jost functions. However, for sufficiently large r (larger than the scale of the background, say $r > 15$ in the examples shown in Fig. 1), Eq. (36) provides a good approximation. In the considered case the background approaches its asymptotic values with exponential speed. In the same way the difference between the Jost function and the approximation (36) is small.

The regular solutions $\Psi(r)$ of Eq. (7) are defined as becoming proportional to the free solutions for $r \rightarrow 0$ and can be expressed in terms of Bessel function,

$$\Psi(r) \sim \left(\frac{k}{q} \right)^{\nu + \frac{1}{2}} \begin{pmatrix} \sqrt{p_0 + m_0} J_{\nu \pm \frac{1}{2}}(qr) \\ \pm \sqrt{p_0 - m_0} J_{\nu \mp \frac{1}{2}}(qr) \end{pmatrix} \quad (37)$$

with $q = \sqrt{k^2 - m_e^2 + m_0^2}$. We introduced for a moment $m_0 = \mu(0)$ which corresponds to a more general case. In all examples considered below we will have $m_0 = 0$. Note also the factor in front which provides the correct normalization.

In order to actually carry out a numerical integration of Eq. (7) it is useful to change to functions with regular initial values at $r = 0$. At once, we must change to imaginary momenta. So we substitute $k \rightarrow ik$ and we make the ansatz

$$\Psi^{(+)} = i^\nu \begin{pmatrix} i\sqrt{p - im_0} \phi_1^{(+)} \\ \sqrt{p + im_0} \phi_2^{(+)} \end{pmatrix}, \quad \Psi^{(-)} = i^\nu \begin{pmatrix} \sqrt{p - im_0} \phi_1^{(+)} \\ -i\sqrt{p + im_0} \phi_2^{(+)} \end{pmatrix}. \quad (38)$$

The equations for $\phi^{(\pm)}$ are

$$\begin{pmatrix} -(p + i\mu(r)) e^{i\theta} & , & \frac{\partial}{\partial r} - \frac{\nu-1/2-v(r)}{r} \\ \frac{\partial}{\partial r} + \frac{\nu+1/2-v(r)}{r} & , & -(p - i\mu(r)) e^{-i\theta} \end{pmatrix} \phi^{(+)} = 0 \quad (39)$$

and

$$\begin{pmatrix} -(p + i\mu(r)) e^{i\theta} & , & \frac{\partial}{\partial r} + \frac{\nu+1/2+v(r)}{r} \\ \frac{\partial}{\partial r} - \frac{\nu-1/2+v(r)}{r} & , & -(p - i\mu(r)) e^{-i\theta} \end{pmatrix} \phi^{(-)} = 0 \quad (40)$$

with $e^{i\theta} = \sqrt{(p + im_e)/(p - im_0)}$. Further we substitute

$$\phi^{(+)} = \left(\frac{qr}{2}\right)^{\nu-\frac{1}{2}} \frac{1}{\Gamma(\nu + \frac{1}{2})} \begin{pmatrix} \frac{qr}{2\nu+1} g_1^{(+)} \\ g_2^{(+)} \end{pmatrix} \quad (41)$$

and

$$\phi^{(-)} = \left(\frac{qr}{2}\right)^{\nu-\frac{1}{2}} \frac{1}{\Gamma(\nu + \frac{1}{2})} \begin{pmatrix} g_1^{(-)} \\ \frac{qr}{2\nu+1} g_2^{(-)} \end{pmatrix}. \quad (42)$$

The boundary conditions at $r = 0$ for these functions are

$$g_{(1,2)}^{(\pm)}(r)|_{r=0} = 1 \quad (43)$$

and they obey the equations

$$\begin{pmatrix} -(p + i\mu(r)) \frac{qr}{2\nu+1} e^{i\theta} & , & \frac{\partial}{\partial r} + \frac{v(r)}{r} \\ \frac{\partial}{\partial r} + \frac{2\nu+1-v(r)}{r} & , & -(p - i\mu(r)) \frac{2\nu+1}{qr} e^{-i\theta} \end{pmatrix} \begin{pmatrix} g_1^{(+)} \\ g_2^{(+)} \end{pmatrix} = 0, \quad (44)$$

$$\begin{pmatrix} -(p + i\mu(r)) \frac{2\nu+1}{qr} e^{i\theta} & , & \frac{\partial}{\partial r} + \frac{2\nu+1+v(r)}{r} \\ \frac{\partial}{\partial r} - \frac{v(r)}{r} & , & -(p - i\mu(r)) \frac{qr}{2\nu+1} e^{-i\theta} \end{pmatrix} \begin{pmatrix} g_1^{(-)} \\ g_2^{(-)} \end{pmatrix} = 0. \quad (45)$$

The above mentioned symmetries can be seen in this representation explicitly. The Jost functions read now

$$f_\nu^{(+)}(ik) = \frac{r(qr/2)^{\nu-\frac{1}{2}}}{\Gamma(\nu + \frac{1}{2})} \left(\frac{qr}{2\nu+1} w g_1^{(+)}(r) K_{\nu-\frac{1}{2}-\delta}(kr) + w^* g_2^{(+)}(r) K_{\nu+\frac{1}{2}-\delta}(kr) \right) \quad (46)$$

and

$$f_\nu^{(-)}(ik) = \frac{r(qr/2)^{\nu-\frac{1}{2}}}{\Gamma(\nu+\frac{1}{2})} \left(w g_1^{(-)}(r) K_{\nu+\frac{1}{2}+\delta}(kr) + \frac{qr}{2\nu+1} w^* g_2^{(-)}(r) K_{\nu-\frac{1}{2}+\delta}(kr) \right) \quad (47)$$

with $w = \sqrt{(p+im_e)(p-im_0)}$ and modified Bessel functions. Eqs. (44) and (45) together with the boundary conditions (43) can be solved easily numerically. We used the package `NDSolve` in `Mathematica`.

Next we need the asymptotic part of the Jost function. We use Eq. (24) with the coefficients X_{nj} , Eq. (25). The integrals over r are convergent and can be calculated numerically without any problems. Taking into account the mentioned symmetries we drop all contributions which are odd under $v \rightarrow -v$ and we define the subtracted logarithm of the Jost function as

$$\ln f^{\text{sub}} = \frac{1}{2} \Re(\ln f_\nu^{(+)}(ik) + \ln f_\nu^{(-)}(ik)) - \ln f_\nu^{\text{as}}. \quad (48)$$

This expression we insert into \mathcal{E}^f , Eq. (21). After integration by parts we arrive at

$$\mathcal{E}^f = \sum_{\nu=\frac{1}{2}, \frac{3}{2}, \dots} \mathcal{E}_\nu^f \quad (49)$$

with the contributions from the individual orbital momenta,

$$\mathcal{E}_\nu^f = \int_{m_e}^{\infty} dk \mathcal{E}_\nu^f(k), \quad (50)$$

and the integrands

$$\mathcal{E}_\nu^f(k) = -\frac{2}{\pi} k \ln f^{\text{sub}}. \quad (51)$$

As illustration of the convergence we show $\mathcal{E}_\nu^f(k)$ enhanced by a factor of $k^3 \nu^3$ in Fig. 2 for several first ν . It is seen that all curves approach the same limiting value which is essentially given by the next term in the uniform asymptotic expansion of the logarithm of the Jost function after that included into $\ln f^{\text{as}}$, Eq. (19) taking into account that the order $\frac{1}{\nu^4}$ is absent for symmetry reasons and the order $\frac{1}{\nu^5}$ is the next one. In this way the integrals over k are fast convergent.

In Fig. 3 we show the contributions from the individual orbital momenta. The corresponding sum in Eq. (49) is also fast convergent and it is sufficient to take a quite small number of the first orbital momenta.

We would like to add a note on bound states. They appear for imaginary momenta, $k = i\kappa$, in Eq. (7), in the region where $p_0 = \sqrt{m_e^2 - \kappa^2}$ is real, $0 < p_0 < m_e$. For such momenta the representation (36) for the Jost function can be rewritten in the form

$$f_\nu^{(\pm)}(i\kappa) = - \lim_{r \rightarrow \infty} r i^{-\nu \mp (\frac{1}{2} - \delta)} \left\{ \sqrt{-p_0 + m_e} \Psi_1(r) K_{\nu \mp (\frac{1}{2} + \delta)}(\kappa r) + \sqrt{p_0 + m_e} \Psi_2(r) K_{\nu \pm (\frac{1}{2} + \delta)}(\kappa r) \right\}. \quad (52)$$

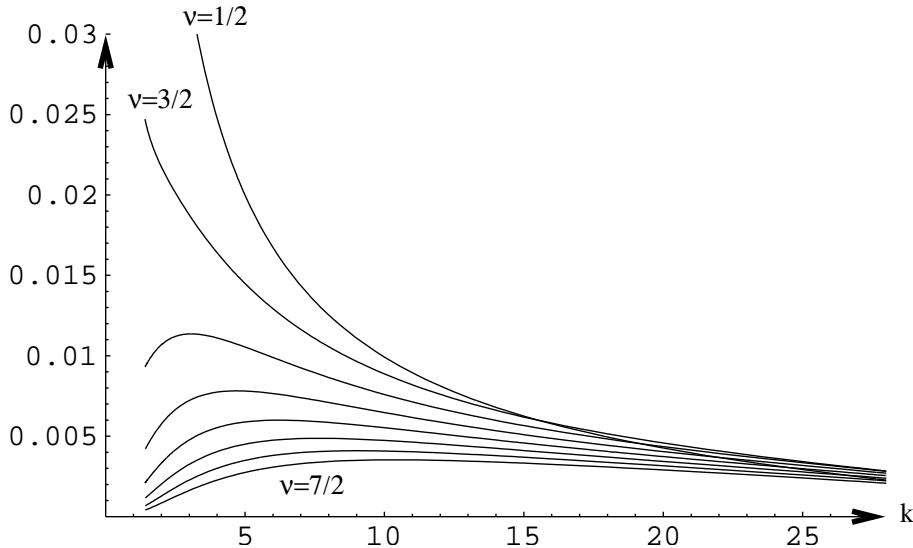


Figure 2: The integrand $\mathcal{E}_\nu^f(k)$ in Eq. (50) multiplied by $k^3\nu^3$ as a function of k for several first values of ν . In this figure and in the next two the parameters are $\beta = 0.3$, $q = 0.5$, $f_e = 1$, $\eta = 1$.

The functions $\Psi_{1,2}$ are solutions of the Eqs. (7) with the initial conditions (37). As both, equation and initial conditions are real for the considered momenta the solutions are also real. In this way the expression in the figure brackets in Eq. (52) are real. Their zeros just determine the location of the bound states. As an example we plot in Fig. 4 these functions for the two lowest orbital momenta. For orbital momentum $m = 0$ we see one bound state, for negative, $m = -1$, none. The appearance of the bound states can be explained easily. Without scalar potential, i.e., for a constant $\mu(r) = m_e$ the spinor moves in a pure magnetic field and in the state where the magnetic moment is antiparallel to the magnetic field its coupling just compensates the lowest Landau level resulting in a zero mode known from [21]. Switching on the scalar potential the spinor feels an additional attraction and becomes a bound state. As concerns the vacuum energy these bound states are outside of the integration region in Eq. (10) and therefore they do not complicate the calculations. As shown in [2] they are accounted for automatically in the representation of the vacuum energy in terms of the Jost function. The only we have to take care of is a possible appearance of bound states on the imaginary k -axis in Eq. (10) above m_e . This would require a zero of the Jost functions in representation (46) or (47) for real k there. But these are genuine complex expressions and it can be shown that they do not have such zeros.

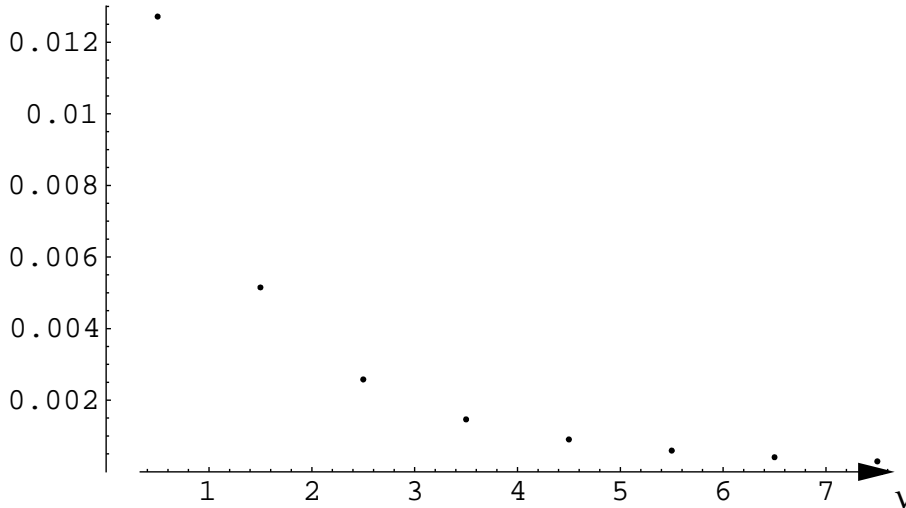


Figure 3: The contributions from the individual orbital momenta \mathcal{E}_ν^f to \mathcal{E}^f in Eq. (49).

	E_{mag}	E_{cov}	E_{scal}	E_{class}
$\beta = 0.3$	0.47913	1.50653	1.91653	3.90220
$\beta = 6$	0.97224	2.64606	3.88896	7.50726

Table 1: Two examples for the classical energy and its constituent parts for $q = 0.5$, $\eta = 1$.

5 Numerical results

We investigated numerically the vacuum energy for values of β ranging from $\beta = 0.3$ to $\beta = 6$ for some choices of the remaining parameters. The convergence properties of the sums and integrals involved have been discussed in the previous section. Here, let us first discuss the weight of the individual contributions.

We start with the classical energy which is given by Eq. (5). It can be divided into three parts. The first one, E_{mag} , is the energy of the magnetic field. The second one, E_{cov} , results from the covariant derivative in Eq. (1) and is given by the second and the third contributions in (5). The third one, E_{scal} , is the self energy of the Higgs and is given by the fourth contributions in (5). We show in Table 1 two examples, one for smallest coupling of the scalar, $\lambda = \beta q^2/2$ and the other for the largest value considered. In both cases as well as in all intermediate ones, the scalar self energy contribution is larger than the magnetic energy and than E_{cov} .

Next we consider for the parameters $q = 0.5$, $f_e = 1$, $\eta = 1$ the constituent parts of the asymptotic part of the vacuum energy, i.e., the $\mathcal{E}_j^{\text{as}}$ as defined in Eq. (33). These quantities are shown in Table 2. As it can be seen the contributions $\mathcal{E}_5^{\text{as}}$ and $\mathcal{E}_6^{\text{as}}$ are dominating. They result from the scalar background, see Eq. (30).

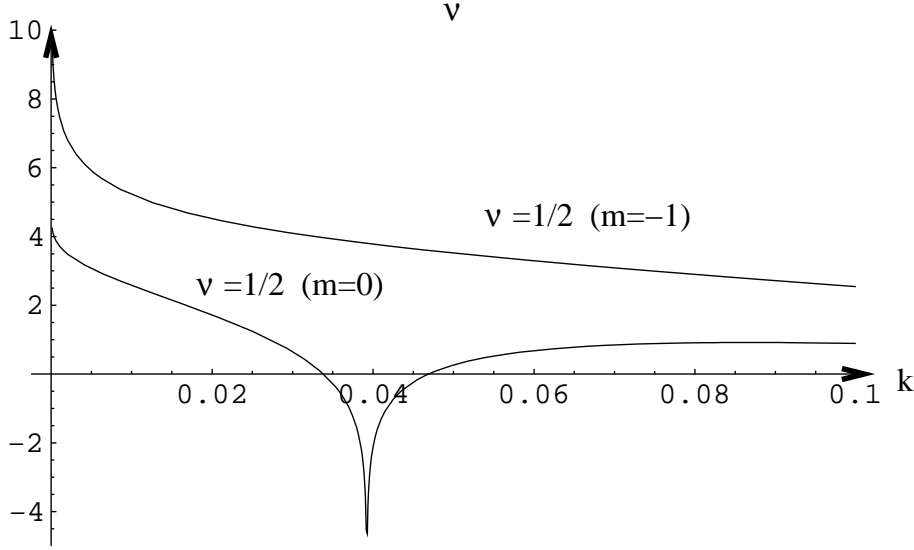


Figure 4: The logarithm of the expressions in the figure brackets in Eq. (52) as function of κ for lowest orbital momenta. The peak indicates a bound state. Its location is $k = 0.039232$.

	$\mathcal{E}_1^{\text{as}}$	$\mathcal{E}_2^{\text{as}}$	$\mathcal{E}_3^{\text{as}}$	$\mathcal{E}_4^{\text{as}}$
$\beta = 0.3$	0.00009139	-0.00006497	$-5.5701 \cdot 10^{-8}$	0.00001052
$\beta = 6$	0.0004916	-0.0003590	$-1.1546 \cdot 10^{-6}$	0.00004194
	$\mathcal{E}_5^{\text{as}}$	$\mathcal{E}_6^{\text{as}}$	$\mathcal{E}^{\text{as}} = \sum_{j=1}^6 \mathcal{E}_j^{\text{as}}$	
$\beta = 0.3$	-0.004379	-0.0017591	-0.0061022	
$\beta = 6$	-0.003898	-0.002483	-0.006208	

Table 2: the constituent parts of the asymptotic part of the vacuum energy for $q = 0.5$, $f_e = 1$, $\eta = 1$.

But generally, all have at least a numerical smallness of two orders of magnitude.

Now, in Table 3, we represent the result of the calculations of the complete vacuum energy for all considered examples. For two cases we also represent the parts of the vacuum energy as a function of β , see Figs. 5 and 6. From these results it can be seen that there seems to be no general rule which part of the vacuum energy is dominating and which not. Moreover, in dependence on the parameters one part may be larger than other and smaller as well. It is even impossible to say something definite about the sign of the vacuum energy, it may change although in most cases it is negative.

q	β	f_e	η	E_{class}	$\mathcal{E}_1^{\text{as}}$	\mathcal{E}^{f}	$\mathcal{E}_{\text{ren}} = \mathcal{E}^{\text{as}} + \mathcal{E}^{\text{f}}$
0.5	0.3	1	1	3.902	-0.006102	0.02410	0.01800
0.5	0.6	1	1	4.549	-0.006102	0.01590	0.009795
0.5	1.	1	1	5.099	-0.006104	0.01153	0.005421
0.5	3.5	1	1	6.710	-0.006146	0.004224	-0.001922
0.5	6.	1	1	7.507	-0.006208	0.001884	-0.004325
1.	0.3	1	1	2.465	-0.005766	0.008686	0.002920
1.	0.6	1	1	2.829	-0.005665	0.005322	-0.0003436
1.	1.	1	1	3.142	-0.005594	0.003030	-0.002565
1.	3.5	1	1	4.093	-0.005593	-0.002588	-0.008181
1.	6.	1	1	4.591	-0.005792	-0.005077	-0.01087
2.	0.3	1	1	2.105	-0.003170	-0.001883	-0.005053
2.	0.6	1	1	2.399	-0.002891	-0.007285	-0.01018
2.	1.	1	1	2.652	-0.002924	-0.01182	-0.01475
2.	3.5	1	1	2.652	-0.002924	-0.02451	-0.02743
2.	6.	1	1	3.861	-0.006539	-0.03022	-0.03676
0.5	0.3	0.1	0.1	0.03902	-0.00006102	$-9.589 \cdot 10^{-6}$	-0.00007061
0.5	0.6	0.1	0.1	0.04549	-0.00006102	-0.00001214	-0.00007316
0.5	1.	0.1	0.1	0.05099	-0.00006104	-0.00001421	-0.00007525
0.5	3.5	0.1	0.1	0.06710	-0.00006146	-0.00001975	-0.00008121
0.5	6.	0.1	0.1	0.07507	-0.00006208	-0.00002216	-0.00008425
0.5	0.3	0.1	1	3.902	-0.0003003	-0.0009589	-0.001259
0.5	0.6	0.1	1	4.549	-0.0005062	-0.001214	-0.001720
0.5	1.	0.1	1	5.099	-0.0007110	-0.001421	-0.002132
0.5	3.5	0.1	1	6.710	-0.001423	-0.001975	-0.003398
0.5	6.	0.1	1	7.507	-0.001814	-0.002216	-0.004030

Table 3: The constituent parts of of the vacuum energy for all considered examples.

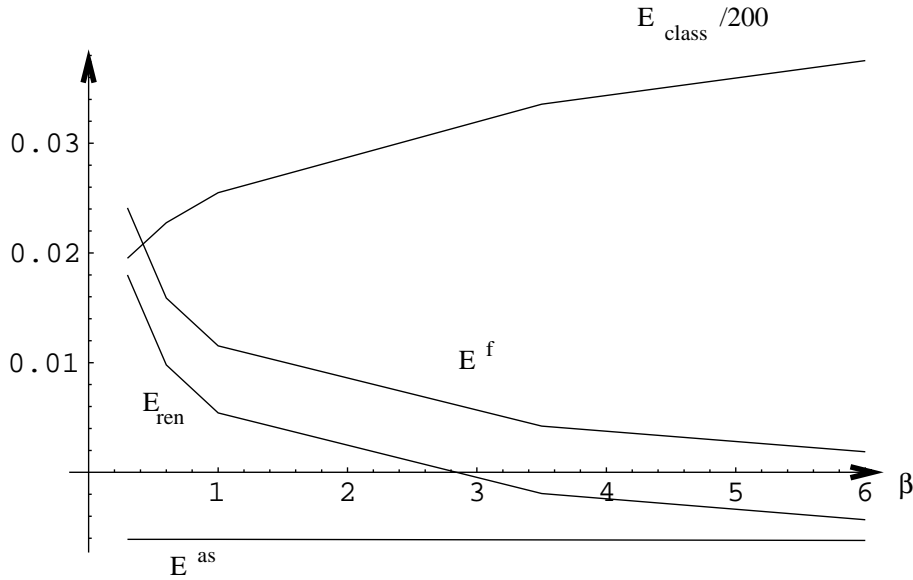


Figure 5: The vacuum energy as a function of β for the $q = 0.5$, $f_e = 1$, $\eta = 1$. In order to represent all quantities within one plot the classical energy is divided by 200.

6 Conclusions

In the present paper we calculated numerically the vacuum energy of a fermion in the background of a Nielsen-Olesen string. As for renormalization we used standard zeta functional regularization and determined the counter terms from the first heat kernel coefficients (up to a_2). It turned out that from the renormalization a counter term appears which is not present in the initial action. It is gauge invariant and it has the correct dimension but it represents a non polynomial interaction. This has to be considered together with the non polynomial interaction present in the model itself as discussed in Sect. 2.

The numerical investigations have been performed using methods developed in the papers [2, 1]. In the present paper the background is given purely numerically in difference to the previous papers where it had been given analytically, for example as a step function or some Gaussian profile. It has been demonstrated that the computational scheme used here is well suited to work with such backgrounds. This is a step forward to physically really interesting problems. In the considered model the stability of the background is given by topological arguments and for a realistic choice of the parameters the quantum contribution is small. This smallness has two sources. The one is the smallness of the coupling constants which appears in front of the quantum contribution relative to the classical one. The second one is a purely numerical smallness of about two orders of magnitude as discussed in Sect. 5. It is present even if the parameters and couplings are all of order one. It is obviously connected with the dimension

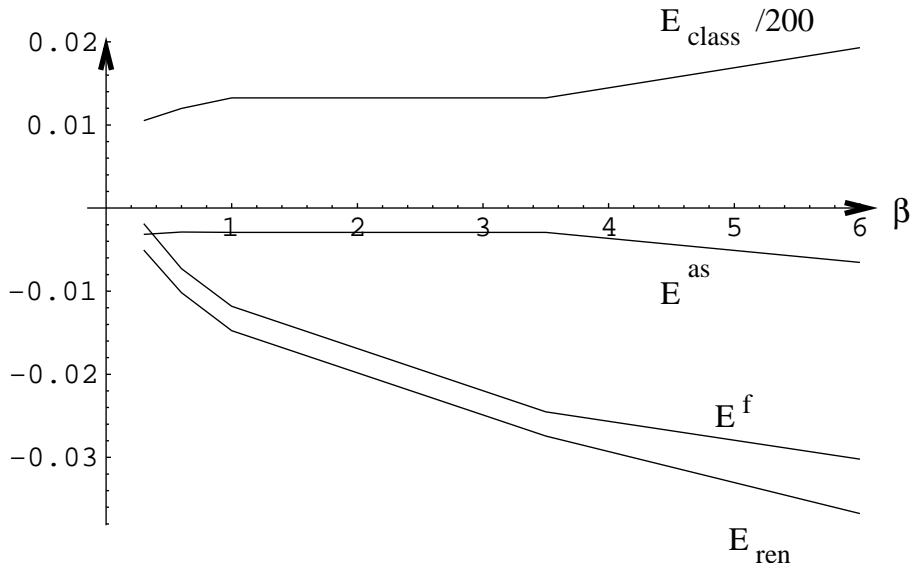


Figure 6: The same as in figure 5 but for $q = 2$.

and the ultraviolet renormalization. So in [12] it was found for a one dimensional background that in (1+1) dimension the vacuum energy is by one order of magnitude larger than for the same problem in (3+1) dimensions. Comparing formulas (29) and (32) in [12] the interpretation is suggested that this difference is due to the one additional ultraviolet subtraction in the (3+1) dimensional case.

As seen in Sect. 5, for the dependence of the vacuum energy on the various parameters no general rule can be seen so far. Even the sign of the vacuum energy changes. The same applies to the relative weight of the individual contributions. So sometimes the asymptotic part is dominating, in other cases, however, the 'finite' part is larger. In general, they are of the same order. From this one can conclude only that in the given background there is no small parameter which could allow for some approximative scheme. So for instance, if the asymptotic part is dominating one could hope to get a good approximation by including higher orders of the uniform asymptotic expansion of the Jost function into the asymptotic part of the vacuum energy and neglect the 'finite' part of it which is the numerically much harder part of the problem. The examples in [13] have been of a kind suggesting this way in contrast to the example in the present paper.

For the considered model of a spinor in the background of the Nielsen-Olesen vortex, due to its smallness, the vacuum energy has only a very small influence on the dynamics of the background. Hence in the considered case the vacuum energy is of limited physical importance. However, its calculation gave new insights into the structure of such calculations and demonstrated the power of the methods used. A next step could be to apply them to the Z and electroweak strings where the stability is not guaranteed by topological arguments and where the stability issue is not finally settled with respect to the fermion contributions [20, 17].

Acknowledgments

The authors are deeply indebted to V. Skalozub for valuable discussions especially in an early stage of the work. Further they thank V. Nikolaev for discussions on the numerical calculation of the background and D. Vassilevich for helpful discussions and suggestions.

One of the authors (I.D.) thanks the Graduiertenkolleg *Quantenfeldtheorie* at the University of Leipzig for support.

Appendix

The Abel-Plana formula used in Sec.2 reads

$$\sum_{\nu=\frac{1}{2},\frac{3}{2},\dots} f(\nu) = \int_0^{\infty} d\nu f(\nu) + \int_0^{\infty} \frac{d\nu}{1+e^{2\pi\nu}} \frac{f(i\nu) - f(-i\nu)}{i}. \quad (53)$$

The following formulas are used in the text,

$$\int_m^{\infty} dk (k^2 - m^2)^{1-s} \frac{\partial}{\partial k} t^j = -m^{2-2s} \frac{\Gamma(2-s)\Gamma(s+\frac{j}{2}-1)}{\Gamma(\frac{j}{2})} \frac{\left(\frac{\nu}{mr}\right)^{j-n}}{\left(1+\left(\frac{\nu}{mr}\right)^2\right)^{s+\frac{j}{2}-1}} \quad (54)$$

with $t = 1/\sqrt{1+(kr/\nu)^2}$. They can be easily derived, see also (C3) and (C2) in [1].

References

- [1] M. Bordag and K. Kirsten. *Phys. Rev.*, 60:105019, 1999.
- [2] M. Bordag and K. Kirsten. *Phys. Rev.*, D53:5753–5760, 1996.
- [3] Marco Scandurra. *Phys. Rev.*, D62:085024, 2000.
- [4] I. Drozdov. Vacuum polarization by a magnetic flux of special rectangular form. 2002. hep-th/0210282, *Int. J. Mod. Phys.*, to appear.
- [5] Gerald V. Dunne and Theodore M. Hall. *Phys. Lett.*, B419:322–325, 1998.
- [6] M. P. Fry. *Int. J. Mod. Phys.*, A17:936–945, 2002.
- [7] Pavlos Pasipoularides. *Phys. Rev.*, D64:105011, 2001.
- [8] Pavlos Pasipoularides. The strong magnetic field asymptotic behaviour for the fermion-induced effective energy in the presence of a magnetic flux tube. 2003. hep-th/0301192.

- [9] Kurt Langfeld, Laurent Moyaerts, and Holger Gies. *Nucl. Phys.*, B646:158–180, 2002.
- [10] Dmitri Diakonov. *Mod. Phys. Lett.*, A14:1725–1732, 1999.
- [11] Holger Bech Nielsen and P. Olesen. *Nucl. Phys.*, B61:45–61, 1973.
- [12] M. Bordag. *J. Phys.*, A28:755–766, 1995.
- [13] M. Bordag. *Phys. Rev.*, D67:065001, 2003.
- [14] Noah Graham, Robert L. Jaffe, and Herbert Weigel. *Int. J. Mod. Phys.*, A17:846–869, 2002.
- [15] N. Graham et al. *Nucl. Phys.*, B645:49–84, 2002.
- [16] Dmitri Diakonov and Martin Maul. *Phys. Rev.*, D66:096004, 2002.
- [17] Martin Groves and Warren B. Perkins. *Nucl. Phys.*, B573:449–500, 2000.
- [18] Holger Gies and Kurt Langfeld. *Int. J. Mod. Phys.*, A17:966–978, 2002.
- [19] Holger Gies and Kurt Langfeld. *Nucl. Phys.*, B613:353–365, 2001.
- [20] Ana Achucarro and Tanmay Vachaspati. *Phys. Rept.*, 327:347–426, 2000.
- [21] Y. Aharonov and A. Casher. *Phys. Rev.*, A19:2461–2462, 1979.
- [22] M. Bordag. *Comments on Atomic and Nuclear Physics, Comments on Modern Physics*, 1, part D:347–361, 2000.
- [23] M. Bordag, K. Kirsten, and D. Vassilevich. *Phys. Rev.*, D59:085011, 1999.
- [24] Michael Bordag, Alfred Scharff Goldhaber, Peter van Nieuwenhuizen, and Dmitri Vassilevich. *Phys. Rev.*, D66:125014, 2002.